Fiber web support of the forming wire

Torbjorn Helle
Professor, paper technology, The Norwegian Institute of Technology, Laboratory of Pulp and Paper Technology, N-7034 Trondheim-NTH, Norway

ABSTRACT *Two factors that affect the initial paper web formation are: (a) the optimum geometrical shape of the "frames" formed between crossing strands in the forming surface of the wire and (b) the strand density, quantified as specific fiber-supporting length per unit area. Based on simplified models of fibers and wire structure, a frame form close to a square is considered to be the optimal one even for highly oriented furnishes. The typical frame dimensions of today's commercial wires lie within a range where rather minor changes may result in significant changes in the initial fiber retention. Good qualitative agreement was found between calculated fiber support and first-pass fiber retention.*

KEYWORDS
Fibers
Formation
Forming fabrics
Papermaking
Paper webs

The forming wire has a rather simple and open structure that should satisfy many requirements and even rather conflicting requirements to a large extent. The wire should separate the dispersed solids efficiently from the suspension, it should provide effective drainage, and it should form a paper web with uniform surfaces and without wire mark.

The fiber material that is to be separated consists of fiber particles having length dimensions similar to, and for a large fraction substantially smaller than, the distance across the voids of the wire structure. Consequently, the initial separation of the particles will be sensitive to relatively minor changes in the form and size of the mesh in the forming wire. This sensitivity even applies to the penetration of the fibers into the wire meshes, affecting the drainage efficiency and the degree of wire mark.

Today, the wire designer has a considerable degree of freedom when choosing between wire structures both with regard to strand number (i.e., mesh size) and mesh form.

To achieve a theoretical basis for the choice of an optimal forming surface, one should look into the relationship between the number and distribution of the fiber supporting strands in the wire structure on one hand and the fiber penetration into the voids of the wire surface on the other hand. Furthermore, the wire's efficiency in separating the fibers from the suspension should be related to the strand density and weave pattern (*1*).

The optimum mesh shape of the forming wire

The basis for fiber retention on the wire

A reasonable though questionable basis for a discussion on the fiber penetration into the wire structure is the assumption that the particles in the fiber suspension will penetrate into the structure deep enough to establish a two-point support in a statically stable way. During initial forming, this means that a fiber has to be supported by at least two wire strands. Here the fiber will remain, although still exposed to a fluid drag perpendicular to its axis, along its length. If no such stable support is established for the fiber, then it will penetrate deeper into the wire structure, eventually passing right through it. The shorter the fiber particle, the denser the supporting strands have to be positioned to catch it.

During initial drainage, only the wire strands are present to catch the fibers. The distance between parallel strands will be the critical parameter for those fibers that are to be separated at the top of the wire structure. (Some fibers will be retained deeper in the wire structure.) A fiber may also be retained when supported by two crossing strands.

The deflection of stiff, elastic fibers

One may start by taking the rather formalistic and simplified standpoint of considering the fibers as straight and stiff elastic rods supported by the wire strands and then study which factors will affect the deflection of the fibers between the strands and the size of this deflection. Here, we consider only the case in which the rod is stably supported, and the deflections of its free ends will be ignored.

Figure 1 shows the deflection of the elastic rod, supported at its ends (*2*). We assume a uniform vertical drag along its full length, caused by the draining water.

The deflection increases proportionally to the 4th power of the distance between the fiber supports. The wire should support the fibers in a way that minimizes their deflection in between the strand knuckles. The deflection will involve several types of problems:

1. The fiber deflection will fill wire voids where water is to drain, reducing the drainage efficiency of the wire.
2. The deflection will create a systematically nonuniform sheet topography (i.e., wire mark).

The theoretically ideal form of an opening or "window" in the forming surface of the wire should then be a circle, provided that the orientation of the fibers is random. However, forming wires are woven structures, made from strands having their main directions perpendicular to each other. Such structures will have rectangular "windows" between crossing strands. If the orientation is random, the optimum "window" form will be a square.

This shape for the best window implies the same number of strands per cm in the machine direction and the cross-machine direction. Squares between crossing strands would be achieved only for the two-shed weave pattern, which therefore seems to be the optimal pattern.

Fibers are *not* randomly oriented during paper forming, because the fibers have a dominant MD orientation. A wire strand knuckle oriented in the cross direction will therefore be more efficient for fiber support than will be an MD-oriented knuckle.

1. The deflection of an elastic beam with two-point supports

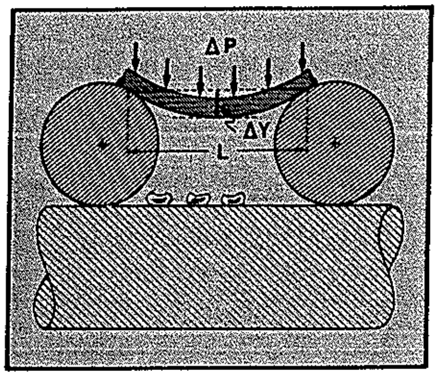

2. In the top strand knuckles of a single-layer wire, the "frame" is always larger than its "window."

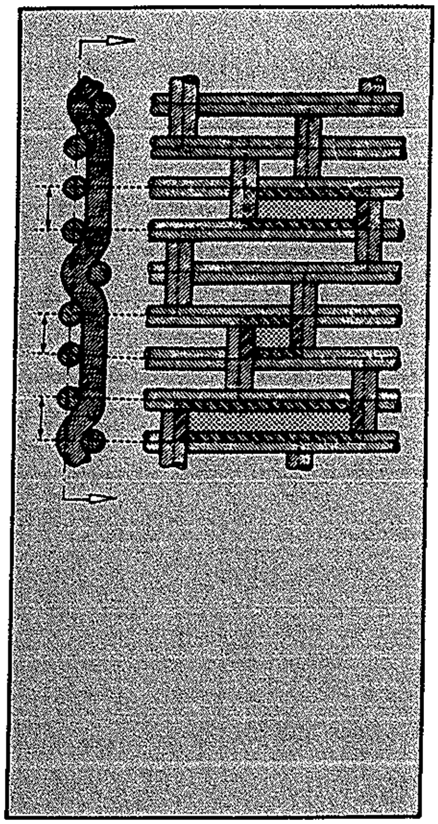

I. Calculated optimal number of chute strands per cm

MD:CD fiber ratio	Chute strands per cm
1:1	30.0
1.25:1	31.75
1.5:1	33.2
2:1	35.4
2.5:1	37.7
3:1	39.5
3.5:1	41.0
4:1	42.4

30 MD strands/cm.

Calculating the optimum frame form

It is difficult, on a theoretical basis, to calculate the optimum form of the strand grid for oriented fibers. However, it is interesting to analyze this calculation, based on some simplified assumptions.

Here, we will use the concepts of wire "frame" and "window." The "frame" is the rectangle defined by the axes of the crossing strands, as shown in **Fig. 2** (shaded areas). The actual open area of the "frame" is termed the "window." (In some literature, the two terms "frame" and "window" may be used as synonyms.) Here, the "frame" will be the critical property, because we can assume that the top of the strand knuckles will dominate as fiber support (depending somewhat on fiber form and stiffness).

A simple, first approximation to a calculation of optimum frame form can be obtained by defining it as that frame form that gives equal amounts of fiber deflection into the frame, for the fibers oriented MD as for those oriented CD. The "amount of fiber deflection" is the product of the number of deflected fibers and the average deflection of these fibers.

Considering only fibers oriented MD and CD, the optimal ratio of length to width of a frame can be calculated and presented as a function of the degree of fiber orientation. **Figure 3** explains the way the calculation is made. The rectangle having sides termed a and $R \cdot a$ represents the frame.

For the calculation of fiber deflection into the frame of Fig. 3, the fraction of the total number of fibers crossing the frame in the machine direction will be termed x, whereas the rest, termed $(1 - x)$, is oriented in the cross direction. (For simplicity, the fibers are assumed to be oriented either in the machine direction or in the cross direction, and the larger fraction is considered to be oriented in the machine direction.)

The deflection Δy of an elastic rod (Fig. 1) is defined by:

$$\Delta y = k\Delta p\,(L^4/EI) \qquad (1)$$

where

Δy = deflection
Δp = specific beam load
L = distance between supports
E = modulus of elasticity
I = moment of inertia.

The amount of fiber deflection (that is, the combined fiber deflection) in the machine direction will be

$$x\Delta y_{MD} = k\Delta p(a^4/EI)x \qquad (2)$$

The amount of fiber deflection in the cross direction is defined as:

$$(1 - x)\,\Delta y_{CD} = k\,\Delta p\,[(R \cdot a)^4/EI](1 - x) \qquad (3)$$

According to the hypothesis, the minimal total deflection will occur when the deflection in either direction equals the other:

$$k\Delta p(a^4/EI)x = k\Delta p\,[(R \cdot a)^4/EI]\,(1 - x) \qquad (4)$$

$$a^4x = R^4a^4\,(1 - x$$

$$R = (x/(1 - x)]^{1/4} \qquad (5)$$

Figure 4 shows the R vs. x relationship. For a wire woven in a two-shed pattern, having an MD (warp) strand number of 30, **Table I** presents the optimum chute number for varying degrees of fiber orientation, based on Eq. 5.

Judged from the standpoint of minimal fiber deflection, the optimum frame form thus does not differ much

3. The frame between the center lines of the crossing strand knuckles

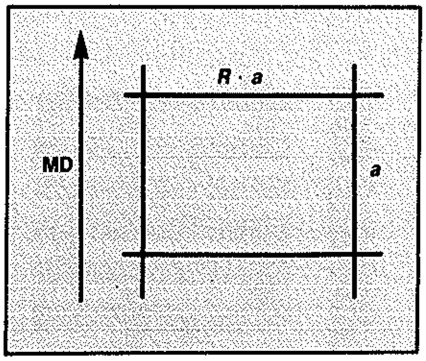

4. Calculated optimal ratio *R* vs. the degree of fiber orientation

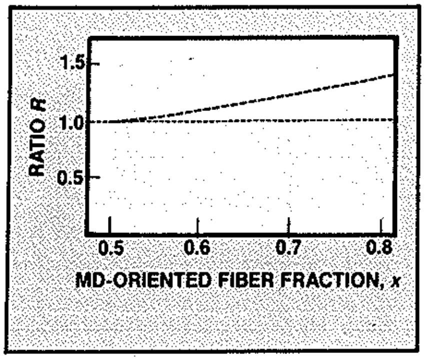

5. Calculated initial retention for model wires having rectangular meshes with different ratios of length to width

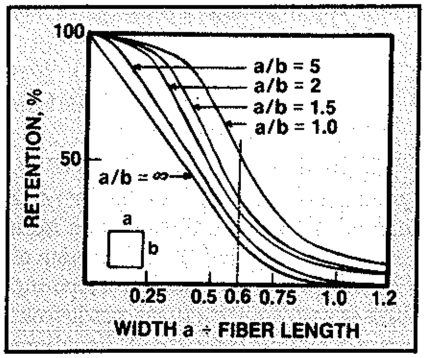

II. Fiber length distribution in mechanical pulps

	Bauer-McNett fiber fraction				
	+28	28/48	48/100	100/200	-200
Weight fraction, %					
Groundwood	15	19	18	16	32
TMP	35	17	14	6	28
Avg. fiber length, mm (weighted average)	2	1.3	0.7	0.4	<0.4

Newsprint pulps with freeness of 90-100 mL CSF.

from a square, even for furnishes of strong fiber orientation. The simple, two-shed weave pattern should therefore provide the best fiber support, even in situations with severe fiber orientation.

Fiber support of the wire and initial retention

The requirements for fiber retention

To provide a two-point support for a fiber on the wire strands, the distance between these two strands obviously has to be less than the length of the fiber.

The number of strands in commercial, single-layer wires normally will be in the range of 20–30 strands/cm in the machine and cross-machine directions, respectively—i.e., 0.5–0.33 mm in center-to-center distance between the strands. Softwood fibers have an average length of 3–3.5 mm, and hardwood fibers have an average length of about 1.0 mm.

During drainage, the fibers will hit the wire with varying angles between (a) their axes and the plane of the wire and (b) their point of gravity at different positions relative to the wire strands. To achieve an appreciable probability of being retained on the wire strands, the fibers therefore have to have a fiber length considerably longer than the center-to-center distance between the strands.

Figure 5 presents the results of a model study performed at The Institute of Paper Chemistry (*3*). In the study, the initial retention was calculated by considering the fibers as solid rods of varying lengths being retained on a mathematical model wire, the "strands" being lines. The "fiber" length was kept in the same length range as the strand-to-strand distance of the theoretical model wire. The ratio of the wire frame edge to the fiber lengths was used as a parameter.

In the study, a two-dimensional wire model having one-dimensional strands was used: that is, the "wire" is a plane grid of lines. Real wires are three-dimensional, of course, and so are the strands.

In Fig. 5, for example, the square frames with edge lengths half the fiber length will give initial retention of some 75%, whereas an increase from 0.5 to 0.6 in the ratio between the frame edge and the fiber lengths will lower the initial retention from some 75% to some 50%.

How, then, does the fiber length distribution of some actual, mechanical pulps fit into this picture? **Table II** provides some data taken from published results (*4*), information from industry (*5*), and our own studies. (*6*).

The ratios between actual fiber lengths and actual strand-to-strand distances are in a range where fiber retention is sensitive to rather minor changes in the strand-to-strand distances.

Specific fiber-supporting knuckle length

To quantify the ability of a given wire to support fibers, a concept termed "specific fiber-supporting knuckle length" is defined as the total length of fiber-supporting strand knuckles per unit area of wire. Only strands in the top strand layer are assumed to be fiber supporting.

Nelson (*3*) does not present actual calculations of fiber-supporting knuckle lengths. The information Nelson gives allows, however, for such calculations. His values for fiber retention can then be correlated with the calculated fiber support numbers. Nelson applies the ratio between fiber mesh dimensions and fiber lengths as a free variable. By using his numbers, a dimensionless expression can be produced, giving a generally valid expression for the fiber support requirement to obtain a certain retention. Then, by inserting the numbers for actual fiber lengths, one may achieve practical values for the relationship between fiber support and fiber retention.

In **Table III**, such a calculation is presented, and required fiber support numbers are calculated for standard fiber lengths of 1 and 3 mm, respectively, at various levels of retention. Some calculated retention and fiber support relationships are presented

6. Calculated relationship between the fiber-support ability and the retention for fibers having uniform lengths of 1 mm and 3 mm

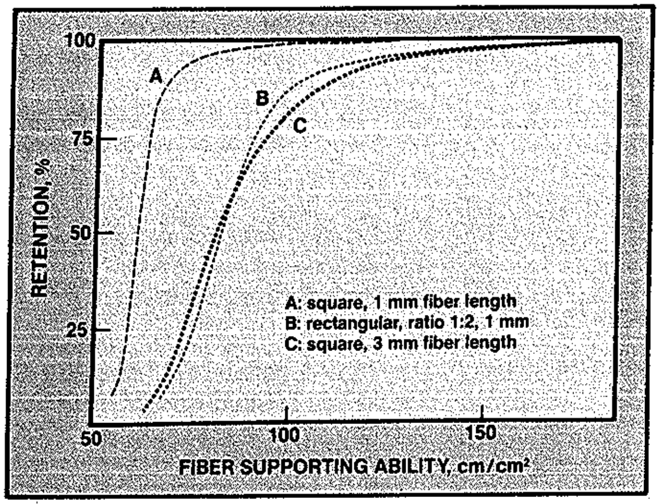

7. Beran's model for single-layered wires used in calculating the fiber support index. **A:** single-layered wire. **B:** strand knuckles of the forming side. **C:** simplified model of the forming wire

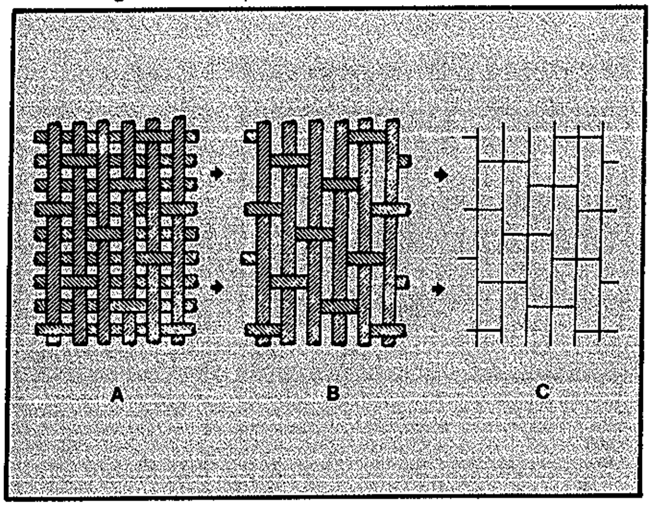

III. Calculation of the relationship between the calculated fiber-supporting length and initial retention of a wire. Square frames of sides a.

	Width a ÷ fiber length											
	0.1	0.2	0.3	0.4	0.5	0.6	0.7	0.8	0.9	1.0	1.1	1.2
Calculated initial retention (3)	0.995	0.974	0.94	0.88	0.74	0.51	0.36	0.24	0.16	0.12	0.1	0.09
Area per frame a^2	0.01	0.04	0.09	0.16	0.25	0.36	0.49	0.64	0.81	1	1.21	1.44
Strand length per frame 2a	0.2	0.4	0.6	0.8	1.0	1.2	1.4	1.6	1.8	2	2.2	2.4
Supporting length per unit area	20	10	6.7	5	4	3.33	2.86	2.5	2.22	2.0	1.84	1.67
Specific supporting length, cm/cm²												
Fiber length 3 mm	66.7	33.3	22.2	16.7	13.3	11.1	9.5	8.3	7.4	6.7	6.1	5.6
Fiber length 1 mm	200	100	67	50	40	33	29	25	22	20	18	17

graphically in **Fig. 6**, based on data given by Nelson (*8*). Judging from Table III and Fig. 6, the retention may be sensitive to rather minor changes in the fiber support length. According to the model, an increase in the fiber support length from 25 to 40 cm/cm², for instance, may increase the initial retention of 1-mm fibers from 25% to 75%.

The question then is how the theoretical calculations and models are related to actual papermaking wires. Knowing the strand numbers and weave pattern of the wires, simple wire models may be drawn that fit the calculation of the fiber supporting ability.

IV. Calculated fiber-supporting lengths for various single-layered wires.

		Fiber-supporting ability, cm/cm²						
		Long warp knuckle side			Long chute knuckle side			Total both sides
Shed no.	Knuckles per cm²	MD	CD	Total	MD	CD	Total	
2	750	30	25	55	30	25	55	110
3	500	30	16.7	46.7	20	25	45	91.7
4	375	30	12.5	42.5	15	25	40	82.5
5	300	30	10	40.0	12	25	37	77

Fiber support index

Beran (*7*) has introduced the concept of "fiber support index" which gives, in principle, the number of fiber support points provided by the wire for a given furnish under technical papermaking conditions. Equation 6 presents the concept as calculated by Beran, based on measured degrees of fiber orientation (*7*):

$$FSI = \pi Z / (2\lambda) = (2/3)(dN_m + 2eN_c) \quad (6)$$

where

FSI = fiber support index
λ = average fiber length
Z = average number of support points under a fiber, provided by the wire
N_m = number of MD wire strands per cm
N_c = number of CD wire strands per cm
d, e = coefficients representing the contributions to fiber support from the MD and CD strands, influenced by weave pattern and running direction.

In the actual calculation of d and e, Beran utilizes the method indicated in **Fig. 7**. Beran's model is directly applicable only for single-layered wires.

Based on the model assumptions of Beran's, it is possible to construct a formula that gives the efficient fiber-supporting knuckle length of any given single-layer wire.

For a d value of 1 and an e value of $2/S$:

$$len_{LW} = (len_{MD} + len_{CD})_{LW} = N_m + 2N_c / S \quad (7)$$

For a d value of $2/S$ and an e value of 1:

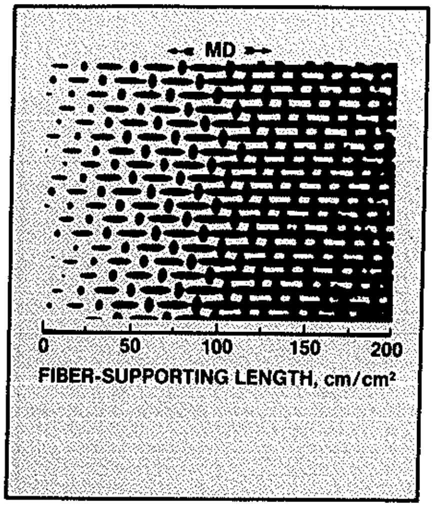

8. Micrograph of the top layer of a single-layered wire

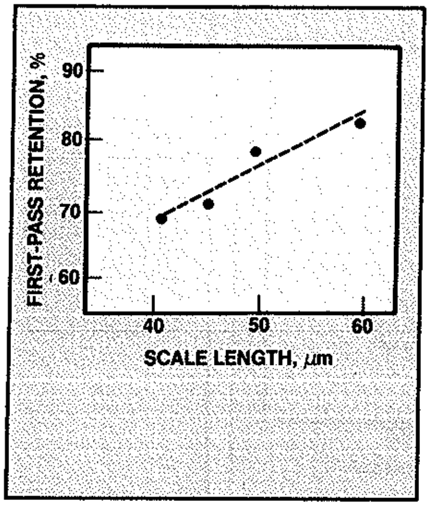

9. Measured first-pass retention in a full-scale trial

V. Calculated fiber-supporting lengths and measured first-pass retention (50% softwood, 50% hardwood chemical pulps)

		Fiber-supporting lengths, cm/cm²					
MD x CD	*Shed no.*	*Nm*	*Nc*	*LWKS*	*LSKS*	*Actual forming side*	*First-pass retention, %*
				Single-layered wire			
32 x 28	5	32	28	32 + 11.2 = 43.2	12.8 + 28 = 40.8	LSKS	68.9
31 x 33	5	31	31	31 + 13.2 = 44.2	12.4 + 33 = 45.4	LSKS	71.2
32 x 37	5	32	32	32 + 14.8 = 46.8	12.8 + 37 = 49.8	LSKS	79.1
				Triple-layered wire*			
30 x 30	2	30	30	30 + 30 = 60	30 + 30 = 60	LWKS	83

*Forming surface woven in two-shed pattern.

$$len_{LS} = (len_{MD} + len_{CD})_{LS} = (2N_m/S) + N_c \quad (8)$$

where

len = total fiber-supporting knuckle length per cm²

LW = long warp knuckle side of the wire

LS = long chute knuckle side of the wire

S = shed number of the wire.

(The formula does *not* give the value of the fiber support index.)

To give actual numbers to the formulas, **Table IV** presents the results of fiber support calculations for various single-layer wires having 30 × 25 strands/cm. In the table, even the numbers of knuckles per cm² are listed. The specific fiber supporting lengths of the wires are in the range of 40–55 cm/cm². Applying these values on the Nelson model of Table III, we would expect an initial retention of some 80% for fibers 1 mm long. This seems to be too high.

Real wires: three dimensional, with curved knuckles

The discussion presented here has been based on the simplified models of single-layer wires shown in Fig. 7. The wires have been assumed to have one-dimensional strands with straight knuckles. However, real wires are constructed by three-dimensional strands. During the weaving and heat setting, the strands are deformed, resulting in noncylindrical strands and curved strand knuckles in the surface of the wires.

The strand shape in the wires may differ considerably from the simplified one based on the weave pattern. It is possible to modify the models of Fig. 7 based on the strand pattern in real wires (*1*). For double-layered wires, the deviation between the theoretical weave pattern and the real shape of the wire structure is so large that it is almost impossible to construct useful models similar to those of single-layered wires.

Figure 8 presents a photograph of the forming side of a single-layered wire. The curved form of the strand knuckles is apparent. In the surface, only the isolated strand knuckles point out. The MD- and CD-oriented knuckles form the complete grid pattern of Fig. 7, only at a depth of some 100 µm under the tops of the knuckles. (100 µm is 1.5 times the thickness of a typical newsprint paper.) Fibers that penetrate that deeply into the wire structure will at least contribute to an undesired wire mark.

Case study: retention achieved in practice as related to calculated fiber support

The calculations presented here have been based on severely simplified models and assumptions. There is an obvious need for a comparison with practical experience.

Tissue paper is assumed to be the grade for which initial retention has the largest effect on the first-pass retention. **Table V** relates the measured first-pass retention achieved during a full-scale trial comparison of a series of wires with the specific fiber-supporting lengths of the forming wires as calculated based on the model of Fig. 7. On a twin-wire machine running at 1200 m/min, the outer, main draining wire is considered (*8*).

Figure 9 depicts the relationship. This is a good qualitative relationship, which indicates that the method for the analysis of fiber supporting length is based on sound principles.

Concluding remarks

The conditions during initial sheet forming are rather complex, in several respects. Water flow movements are parallel to and perpendicular to the forming wire, there are pressure and suction pulsations under the wire, and fibers and other particles deposit onto the wire.

Today's knowledge about the interactions between wire and fiber are almost solely empirical, supplemented by some general qualitative relationships. To improve the design criteria involved in the choice of wire parameters, there is today a need for process models that can bring richer understanding of the mechanisms involved in initial sheet forming.

This study is an attempt in this direction. It has been based on severe simplifications, the validity of which can of course be questioned. The results, however, are in principal accordance with the practical experience for various wire types.

The next step is to develop computer

simulation models for further studies of the quantitative relationship between the fiber support and fiber retention, as well as for the dynamics of the process. Another important expansion of the model is to adjust it for ribbonlike, flexible fibers.

Literature cited

1. Helle, T., Om formingsvirens arkunderstottelsesevne, report submitted to the Royal Norwegian Council for Scientific Research, 1985 (in Norwegian).
2. Helle, T., Preprints 1982 International Water Removal Symposium TS-CPPA, Montreal, p. 93, Vancouver, B.C., Oct. 26, 1982
3. Nelson, R.W., Tappi 47(12): 752(1964).
4. Tasman, J.E., Tappi 55(1): 136(1972).
5. Information provided by S. Aurstad, Norske Skogindustrier.
6. Fiber studies by H. W. Giertz, L. Hegbom, A. Kvitvang, and T. Helle, Pulp and Paper Lab., Norw. Inst. of Techn., Trondheim.
7. Beran, R. L., Tappi 64(4): 39(1979).
8. Swanberg, O., Paper No. 2 in KMN-Nordiskafilts Tissuemaking Seminar papers, Karlstad, Sweden, Aug. 22, 1983.

Received for review Jan. 26, 1987.

Accepted Aug. 21, 1987.

Presented at the 1987 Papermakers Conference.

Pressurized grinding of chemically treated wood

Mikael Lucander

Research Associate, The Finnish Pulp and Paper Research Institute, P. O. Box 136, SF-00101 Helsinki, Finland

ABSTRACT *Mild sulfonation of softwood prior to mechanical defibration yields pulps with enhanced strength properties. Development of the chemigroundwood process has been hampered by the dimensions of the raw material to be impregnated. This study shows that impregnation with sodium sulfite solutions at elevated temperature is successful at short impregnation times. Pressure grinding of the mechanically treated wood did produce CPGW pulps that in many respects are comparable to CTMP. Compared to the reference PGW pulps, the CPGW pulps had a higher long fiber content and 50–100% higher tensile and tear strengths, but optical properties suffered, as expected.*

KEYWORDS
Chemical analysis
Grinding
Mechanical properties
Impregnation
Picea abies
Sulfonation

Interest among paper and linerboard manufacturers in utilizing chemically pretreated, pressurized groundwood (CPGW) is limited. There are a few exceptions, however, such as grinding of hardwoods preimpregnated with sodium carbonate. The principal drawback of the CPGW process as compared with the CTMP process is the long impregnation time required as a result of the size and form of the raw material, which is logs.

Impregnation of wood with alkaline sodium sulfite is relatively easy compared with impregnation of wood with white liquor. Sulfonation takes place at a rather low temperature, and sodium sulfite has proven to be a suitable chemical for producing mechanical pulps, especially CTMP.

Studies on impregnation of Finnish spruce with sodium sulfite followed by pressure grinding of the impregnated wood raw material have been performed on a laboratory scale at the Finnish Pulp and Paper Research Institute. A method for determining the effectiveness of the impregnation under different conditions was developed in conjunction with the study.

1. The experimental program in Series 1

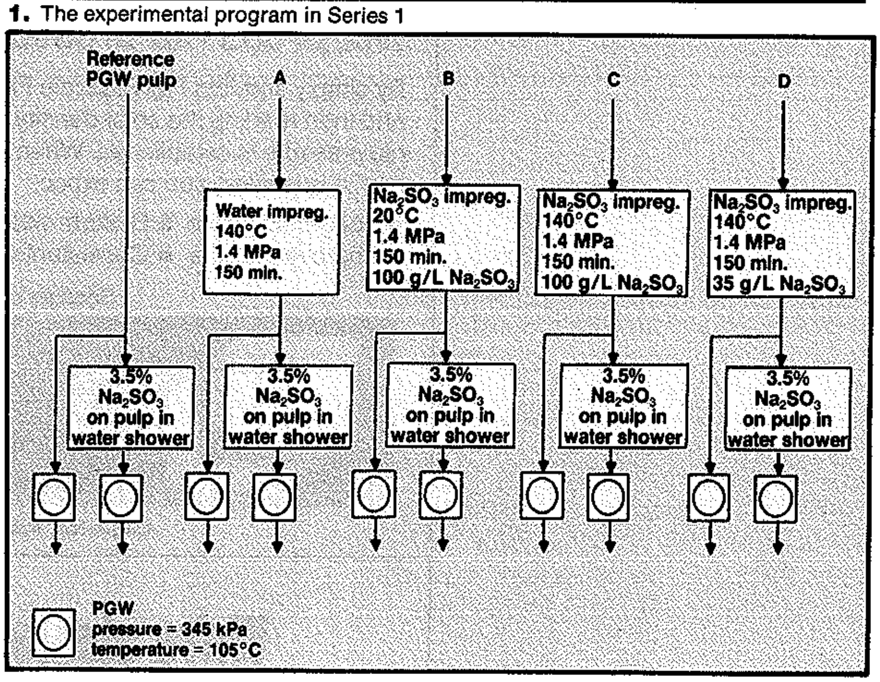

Experimental Program

Impregnation of wood and the subsequent grinding of the sulfonated raw material were studied in two different experimental series. In the first series, comparisons were made between impregnation with hot water, cold sulfite, and hot sulfite at two different concentrations. In addition, the influence of sulfite-containing shower water on the quality of pulps produced as PGW or CPGW was studied. In this series, a long impregnation time of 150 min was used. The experimental program is given in **Fig. 1.**

As shown in **Fig. 2**, four variables were studied in the second series:

1. Vacuum treatment of wood in the impregnation vessel

2. The experimental program in Series 2

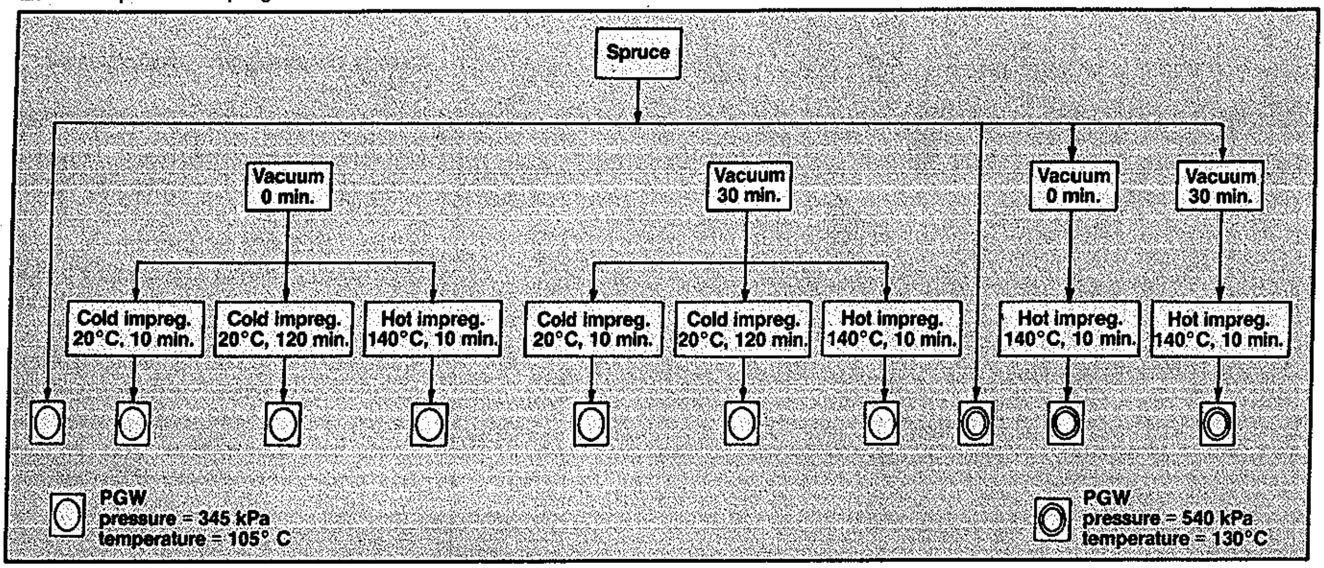

3. Bauer-McNett long fiber fractions of reference and CPGW pulps in Series 1

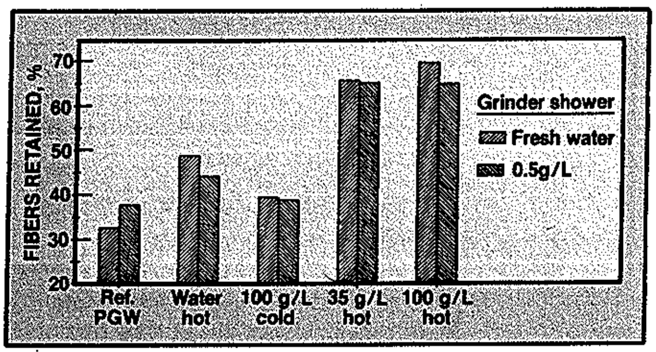

4. Bauer-McNett long fiber fraction of reference and CPGW pulps in Series 2

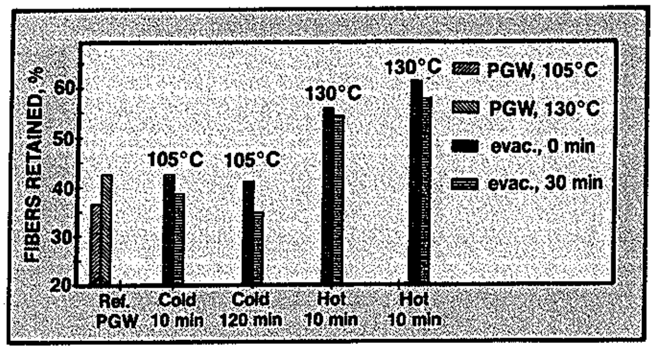

5. Somerville shives of the PGW and CPGW pulps prior to hot disintegration

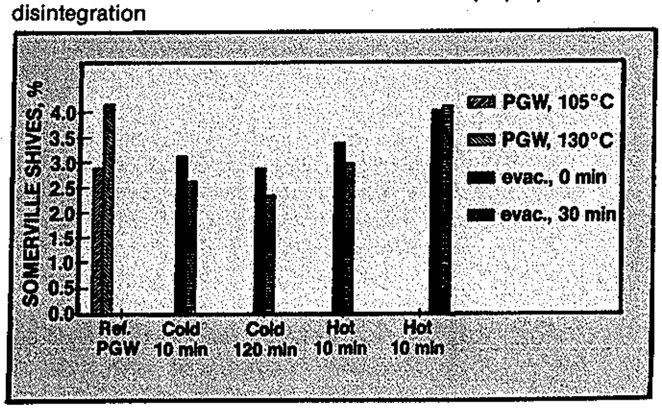

6. Tensile index measured on 52-g/m² laboratory sheets in Series 1

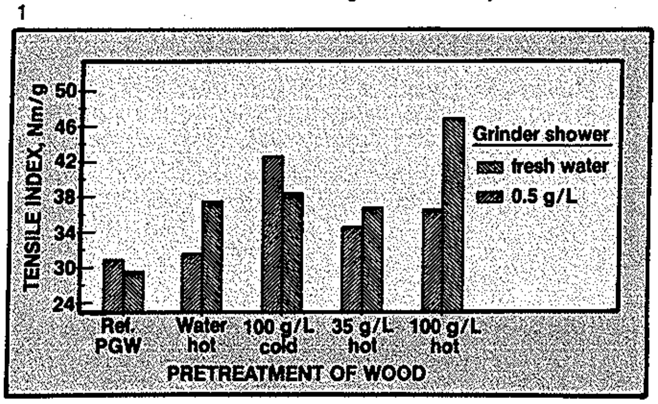

2. Impregnation temperature
3. Impregnation time
4. Grinding temperature.

Results

Sulfur content of impregnated wood and CPGW pulp

Data on analyses of the sulfur content of wood after impregnation and also on the washed pulp in Series 1 are given in **Table I**. The sulfite liquor readily impregnated the wood raw material. The sodium sulfite charge at the two concentrations of 35 g/L and 100 g/L (140°C) resulted in 3% and 9% sulfite contents in the wood respectively, calculated as Na_2SO_3 on o.d. wood.

The sulfur contents in the washed pulps were 0.9% and 2.0%, respectively, expressed as a percentage of sodium sulfite on o.d. pulp. A high sulfite charge was achieved with cold impregnation liquor (100 g of Na_2SO_3 /L)—that is, 7% sodium sulfite on o.d. wood. Washed pulp, however, contained only 0.7% sodium sulfite.

Using sodium sulfite in the shower water (3.5% on wood) increases the sulfur content of the washed pulp. The amount corresponds to sodium sulfite

I. Sodium sulfite content of impregnated wood and washed pulp, Series 1

Trial	Treatment	Impregnation: Na_2SO_3 dosage, g/L	Impregnation: Analyzed Na_2SO_3, % o.d. wood	Grinding: Analyzed Na_2SO_3, % o.d. pulp
1	Ref. PGW	0	...	0.04
2	Ref. PGW*	0	...	0.24
3	Hot water	0	0.1	0.04
4	Hot water*	0	0.1	0.24
5	Cold sulfite	100	7.4	0.67
6	cold sulfite*	100	7.4	0.79
7	Hot sulfite	35	3.3	0.94
8	Hot sulfite*	35	3.3	1.06
9	Hot sulfite	100	8.7	2.00
10	Hot sulfite*	100	8.7	2.08

*Sulfite at a concentration of 0.5 Na_2SO_3/L was added to the shower water.

II. Sodium sulfite content of impregnated wood and washed pulp, Series 2

Trial	Impregnation: Time, min	Impregnation: Temp., °C	Impregnation: Analyzed Na_2SO_3, % o.d. wood	Grinding: Analyzed Na_2SO_3, % o.d. pulp	Grinding: CH_2Cl_2 extract, %
				Shower water 105°C	
1	Ref. PGW	...	0.07	0.04	0.48
2	10	20	3.5	0.56	0.40
3	120	20	4.8	0.67	0.40
4	10	140	4.5	0.91	0.39
5	10*	20	4.2	0.51	0.30
6	120*	20	5.3	0.59	0.32
7	10*	140	6.0	0.99	0.33
				Shower water 130°C	
8	Ref. PGW	...	...	0.04	0.51
9	10	140	4.6	0.99	0.35
10	10*	140	5.6	0.95	0.43

*The wood was vacuum treated prior to impregnation.

contents of 0.2% and 0.1–0.15%, depending on whether untreated or sulfonated wood was ground.

Experiments carried out in the second series (**Table II**), show that vacuum treatment of the wood in the impregnation vessel slightly improves the cold impregnation results (Experiments 2, 3, 5, and 6).

The effect on impregnation efficiency is stronger when impregnating with hot liquor (Experiments 4, 7, 9, and 10). Increasing the impregnation time improves performance when impregnating with cold liquor. The best impregnation results in the study were achieved with hot liquor, as reflected specifically in the sodium sulfite content of the washed pulps, with the numerical results being in the range of 1% sodium sulfite on wood.

In the best cases, dichloromethane extractives were reduced from a concentration of 0.5% to 0.3%.

Energy consumption properties of CPGW pulps

Untreated and chemically treated wood samples had roughly the same specific energy consumption under similar process conditions—1.1±0.2 MW·h/ton (**Tables III and IV**). Because the number of experiments was restricted, no attempt was made to optimize the grinding of the chemically treated wood. The freeness of the CPGW pulps produced in the first series was thus higher than for the reference PGW pulps—300–400 mL and 100–150 mL, respectively. Also, in the second series pulp produced through hot impregnation had a higher freeness than the other pulps in the series, at 200–350 mL compared to 150–250 mL.

The results show that sulfonation of the wood raw material reduces the fiber-to-fiber bonding. The CPGW pulps produced a large amount of unbroken fiber and a small amount of fine fraction material.

Fiber properties of PGW and CPGW pulps

Impregnation of the wood raw material, especially hot impregnation, increased the amount of long fibers. In Bauer-McNett classification, the upper fraction, retained by a 595-μm screen (28 mesh), increased from 40% to 65%. The middle fraction, passing through a 595-μm screen but retained by a 74-μm screen (200 mesh), was reduced by about 50% from the original level of 40%. The fines fraction, passing through a 74-μm screen, was reduced from 25% to 15% on average. These percentages are valid for the first test series (**Fig. 3**).

In the second test series, the influence of hot impregnation was reflected as an increase in the long fiber fraction as compared with data for the PGW reference pulps. The long fiber fraction corresponded to 55–60% and 35–45%, respectively, for the PGW pulps (**Fig. 4**).

The hot impregnation did have a surprisingly modest influence on the amount of Somerville shives, especially in light of the corresponding Bauer-McNett analyses data (**Fig. 5**). The use of hot shower water (130°C) during the grinding operation did, however, increase the shives content by 1%. The Somerville shives contents

III. Experiment results of pressure grinding of sodium sulfite impregnated wood, Series 1

	Impregnation		Grinding	
Trial	Treat-ment	Na_2SO_3 dosage, g/L	Sp. energy consump-tion, MW-h/ton	Freeness, mL CSF
1	ref.	. . .	1.09	110
2	ref.	. . .	1.02	163
3	water	. . .	1.19	192
4	water	. . .	1.30	142
5	cold	100	1.33	95
6	cold	100	1.09	109
7	hot	35	0.91	414
8	hot	35	0.96	293
9	hot	100	0.91	348
10	hot	100	0.97	368

Sulfite at a concentration of 0.5 g Na_2SO_3/L was added to the shower water.

IV. Experiment results of pressure grinding of sodium sulfite impregnated wood, Series 2

	Impregnation		Grinding	
Trial	Time, min	Temp., °C	Sp. energy consump-tion, MW-h/ton	Freeness, mL CSF
			Shower water 105 °C	
1	ref.	. . .	1.08	203
2	10	20	1.02	238
3	120	20	1.03	185
4	10	140	1.05	344
5	10*	20	1.10	165
6	120*	20	0.94	203
7	10*	140	0.97	341
			Shower water 130 °C	
8	ref.	. . .	0.97232	
9	10	140	0.97	311
10	10*	140	1.13	204

*The wood was vacuum treated prior to impregnation.

7. Extrapolated tensile strength values of pulps in Series 1

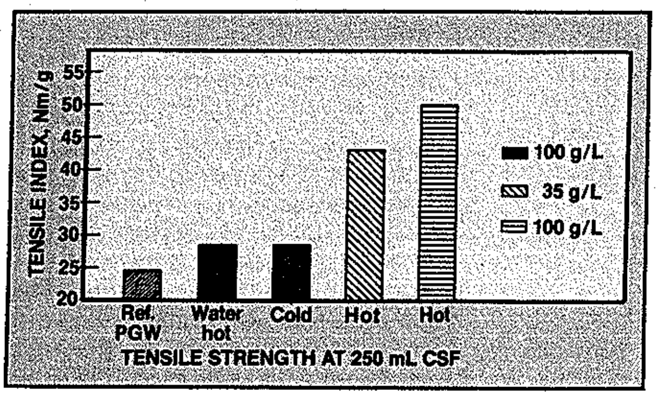

8. Tensile index measured on 52-g/m² laboratory sheets in Series 2

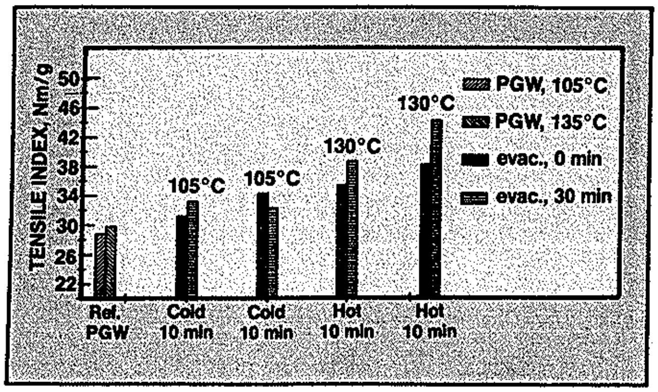

9. Tear index measured on 52-g/m² laboratory sheets in Series 1

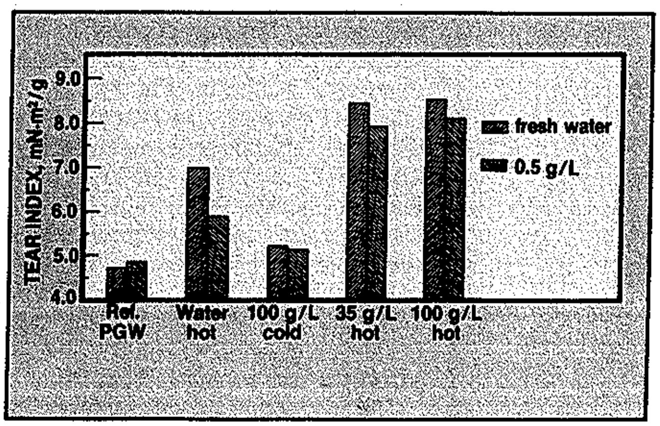

10. Tear index measured on 52-g/m² laboratory sheets in Series 2

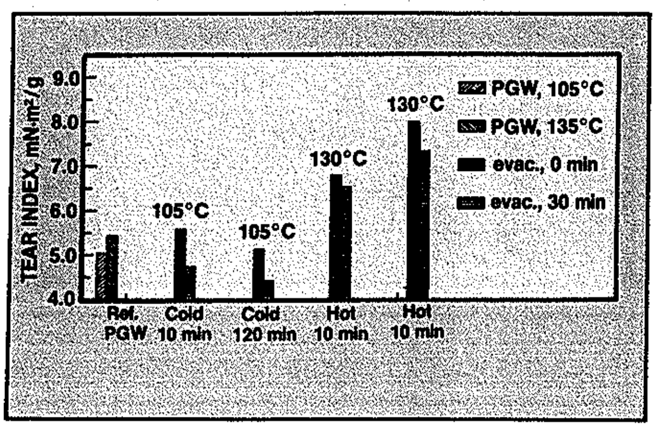

11. Brightness of the PGW and CPGW pulps in Series 2

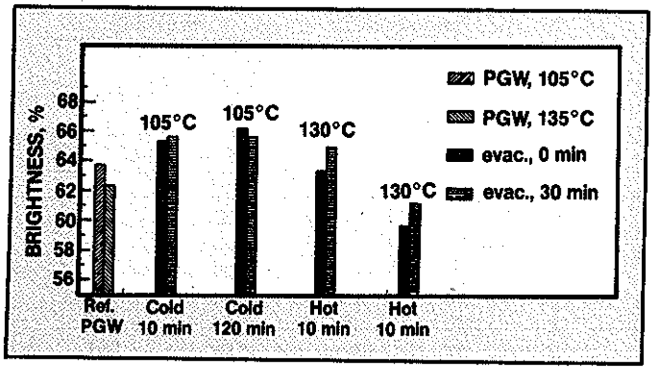

12. Brightness of the PGW and CPGW pulps in Series 1

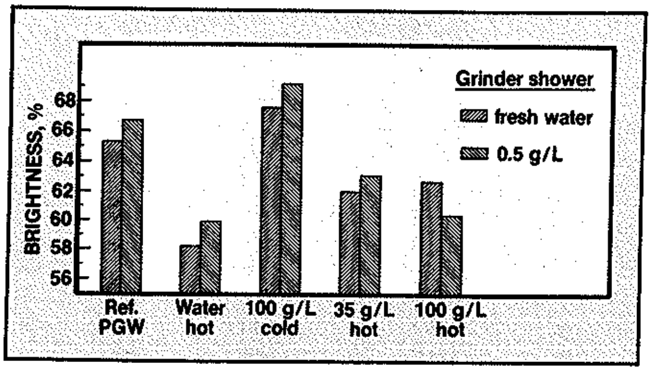

13. Light-scattering coefficient of the PGW and CPGW pulps in Series 1

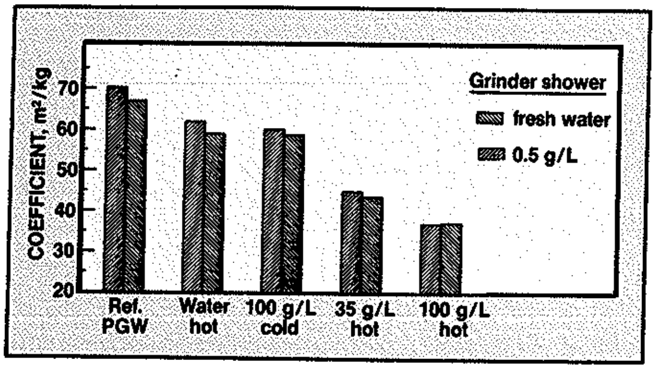

14. Light-scattering coefficient of the PGW and CPGW pulps in Series 2

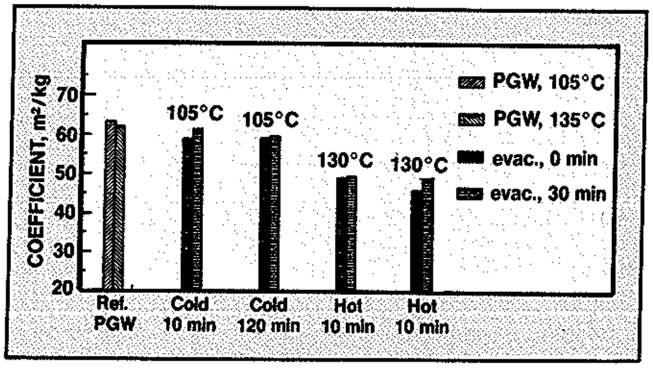

15. Wood handling of the raw material used in this study.

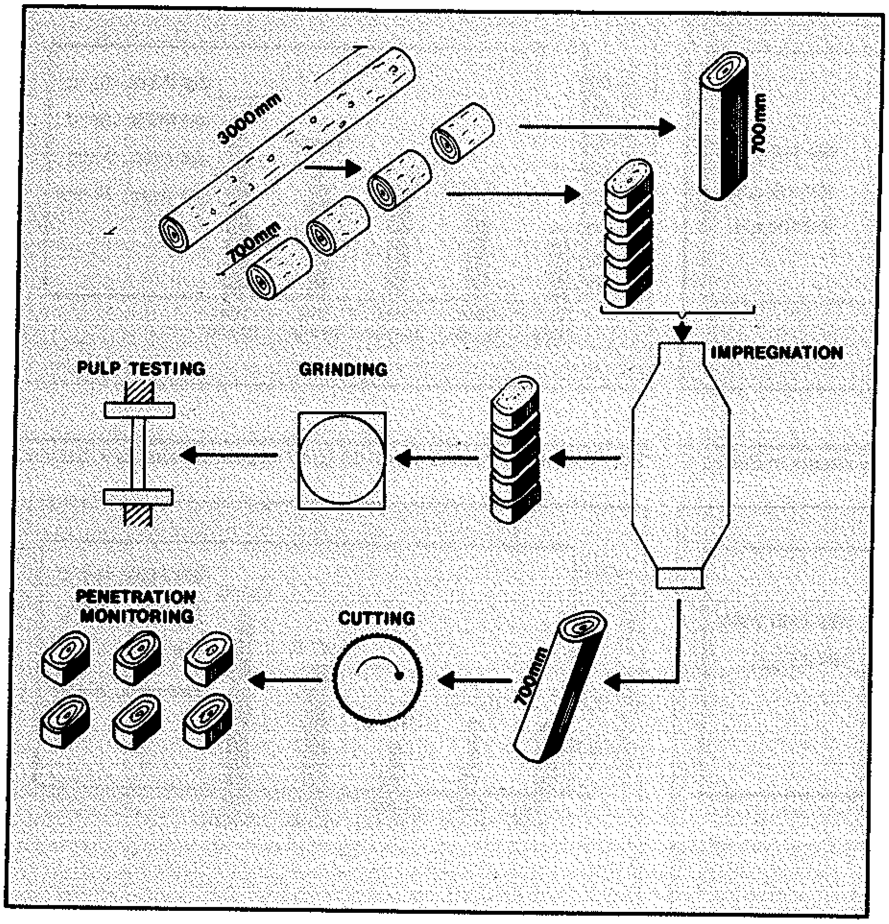

of PGW and CPGW pulps were both reduced to 1.5% after hot disintegration.

Pulp strength properties

The effect of sulfite treatment of the wood raw material is reflected in the strength properties of the pulp. The tensile strength for the CPGW pulps in the first series is high (**Fig. 6**), especially considering the high freeness of the pulps (**Fig. 7**). Hot water impregnation and impregnation with cold sulfite liquor improved the tensile strength of the pulps equally by about 15%, whereas hot impregnation, especially with strong sodium sulfite liquor concentration, doubled the tensile strength figures for the pulp. In both series, impregnation with hot sulfite liquor enhanced the tensile strength of the pulps (**Fig. 8**).

In the first series, tear strength for the CPGW pulps in some cases reached 8 mN·m²/g, compared with 5 mN·m²/g for the reference PGW pulps (**Fig. 9**). Using sulfite in the shower water seems to slightly reduce the tear strength for CPGW pulps. Results from the second series showed that cold impregnation with sulfite did not affect the tear strength (**Fig. 10**).

Hot impregnation did, however, in-

16. The impregnation and grinding scheme in Series 1 (A) and in Series 2 (B)

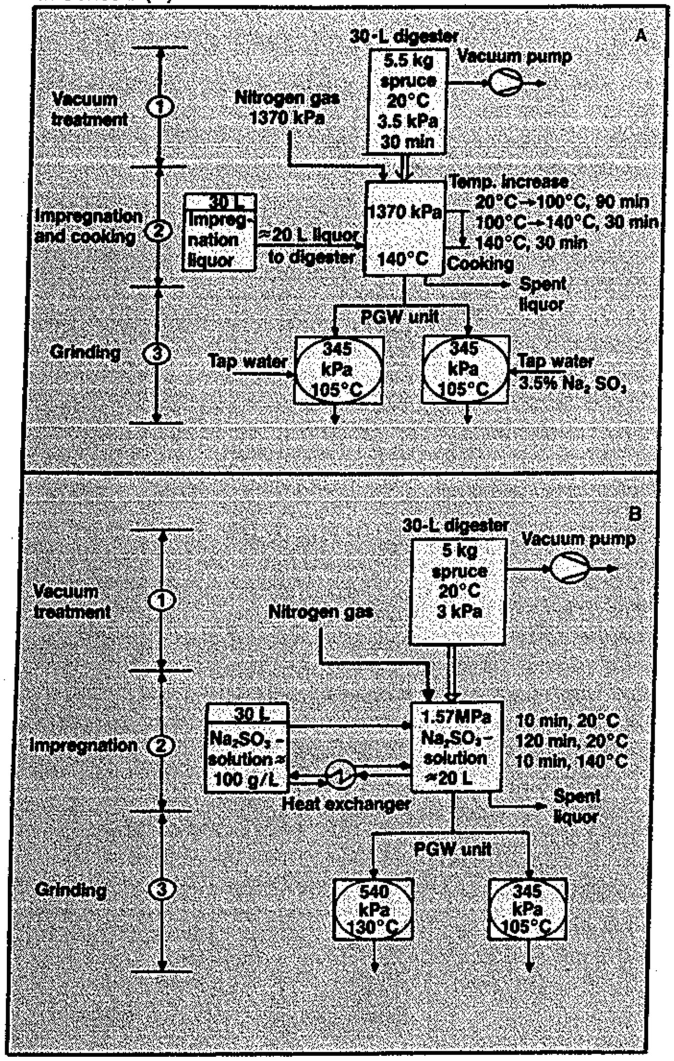

17. The pressurized grinder equipment used in the study

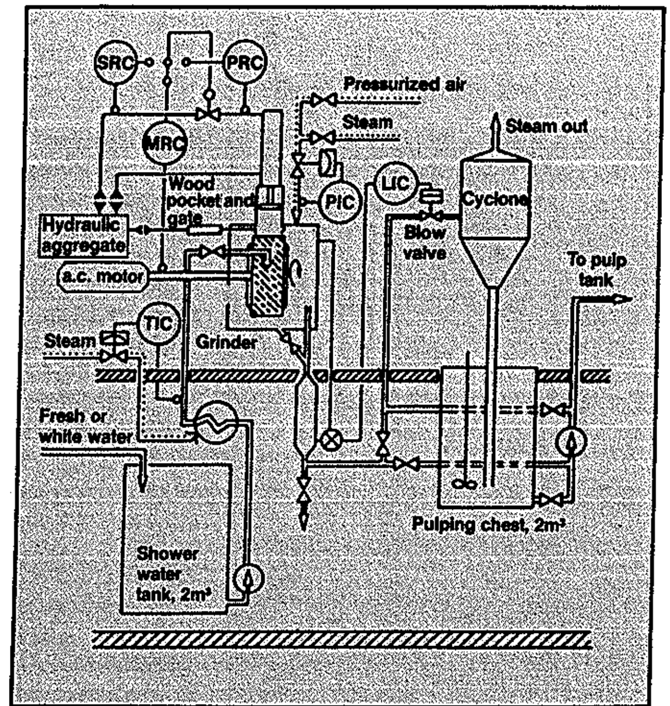

Grinding stone, mm	
width	120
diameter	500
Grinding zone, mm	100 x 150
Peripheral speed, m/s	5–50
Power, kW	110
Grinder casing pressure, kPa	0–500
Production, kg/h	5–50

Hydraulic feed of wood, alternatively at constant grinding pressure, constant grinding rate, and constant motor load.

crease tear strength from STa3–m²/g to 7 mN·m²/g. Vacuum treatment also reduced tear strength.

As expected, the use of hot shower water (130°C) in grinding increased the tear strength for the pulps produced.

Optical properties

Data from Series 2 show that cold impregnation is favorable to pulp brightness. Brightness improved by 2 units (**Fig. 11**). The brightness of pulps produced using hot-impregnated wood was about the same as the brightness of the reference pulps. The combination of hot-impregnated wood and hot shower water yielded pulps with considerably lower brightnesses. The pulp with the highest brightness in Series 1 was produced with cold impregnation. In this series, the long impregnation time of 150 min had a negative effect on the brightness of the CPGW pulps (**Fig. 12**).

The negative effect of the chemical treatment on the light-scattering properties of the pulps was evident.

In Series 1, the light scattering coefficient declined from 70 to 45 and 37, respectively, for mild and strong impregnation liquor concentrations (**Fig. 13**). In Series 2, the light-scattering coefficient declined from 65 for the reference pulps to 50 for pulps produced with hot impregnation (**Fig. 14**).

Conclusions

Sodium sulfite impregnation of wood raw material for subsequent grinding is successful under relatively mild impregnation conditions. This is true even if the wood has rather large dimensions. Impregnation with 140°C liquor for 10 min resulted in fast penetration of the wood by the impregnation liquor. The resulting effect was considerable improvement in pulp properties.

Pressure grinding of chemically treated wood did produce CPGW pulps with properties that in many respects are comparable with CTMP pulps. The Bauer-McNett long fiber fraction and the tear strength for the CPGW pulps improved about 50%, and the tensile strength by 50–100% as compared with the reference pulps, the PGW pulps. As expected, sulfite treatment of the wood had an adverse effect on the light-scattering properties of the pulps. Scattering declined by some 25–50%.

Vacuum treatment of wood raw material in the impregnation vessel improved liquor penetration, but the actual effect on the strength properties of the pulp was negligible. Grinding with a high shower water temperature was especially effective in improving the strength properties of the CPGW pulps.

18. Wood blocks trimmed to fit the grinding zone and sliced for chemical analysis

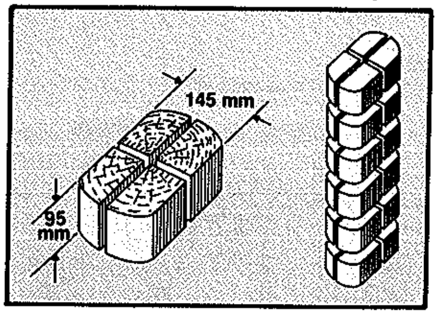

Experimental procedures

Wood raw material

Local spruce (*Picea abies*) was used in the study. The impregnation vessel allowed experiments with log sizes up to a diameter of 180 mm and a length of 700 mm. The experiments aimed at studying the effectiveness of impregnation in logs of a rather large size. Both fresh and partly dried wood was used in the experiments.

The 3-m logs were barked and trimmed on two sides to produce 145-mm-wide beams. (The length of the grinding zone of the unit used is 150 mm.) The beams were cut either into 700-mm-long pieces for the impregnation vessel or into 95-mm-long pieces for grinding, as shown in **Fig. 15.** (The width of the grinding zone is 100 mm.)

Impregnation and cooking

Impregnation and sulfonation of the wood was performed in a 30-L vessel equipped with forced liquor circulation. Phases involved in the chemical treatment were:

1. Filling the vessel with wood
2. Vacuum treatment (optional)
3. Addition of cold (20°C) or hot (140°C) impregnation liquor
4. Pressurizing the vessel using nitrogen gas
5. Cooking (sulfonation), starting either with a temperature raising period or directly from full temperature
6. Removal of the impregnation liquor after the completed cooking phase.

The liquor was circulated through the external heat exchanger in all experiments regardless of the temperature to be achieved. The sodium sulfite concentrations in the liquor were 35 g/L and 100 g/L. The impregnation phases are depicted in **Fig. 16.**

Grinding

The impregnated logs were kept in sealed plastic bags until the actual grinding began. Grinding was performed with the pilot unit facilities available at the Finnish Pulp and Paper Research Institute. The grinder, which can be operated under normal pressure or in a pressurized state, was supplied by Oy Tampella Ab. **Figure 17** depicts the grinding unit. Grinding was performed under the conditions given in **Table V.**

Clean tap water was used to maintain the grinding consistency at 1.4%. A few experiments were done with a sulfite-containing shower at a sodium sulfite concentration of 0.5 g/L. All experiments were performed in the pitless run mode.

Wood and pulp analyses

The impregnated wood species designated for sulfur analyses (**Fig. 18**) were stowed in sealed plastic bags immediately after the impregnation step and before cooling. The cooled wood samples were carefully dried for 24 h at 50°C in an oven equipped with efficient ventilation. The wood samples were cut into 3-cm-wide slices, chipped in a laboratory chipper, dried, and milled. The amount of sodium sulfite penetrating the wood during impregnation was calculated from the total sulfur amount measured in the wood meal samples.

It was possible to monitor the penetration of the wood by sulfite liquor with a relatively simple procedure. After impregnation, the wood beam was cut at different locations perpendicular to the length. The exposed surfaces were colored with suitable pH-sensitive indicator solutions, the best choice being an alizarin–methanol solution.

The pulps were screened using a vibrating laboratory screen with 4 mm holes. The properties of the screened pulps were measured. Strength and optical properties were measured using 52-g/m² sheets prepared with recirculated white water. Dichloromethane extractives was measured on 500-g/m² samples prepared in a Buchner funnel. These samples were not wet-pressed prior to drying.

Thanks to Oy Tampella Ab for assistance and cooperation in carrying out the studies.

Received for review July 17, 1987.

Accepted Aug. 21, 1987.

Presented at the 1987 Pulping Conference Proceedings, a TAPPI PRESS publication.